Dynamic variation in cycling of hematopoietic stem cells in steady state and inflammation

Hitoshi Takizawa,[1,2] Roland R. Regoes,[3] Chandra S. Boddupalli,[1,2] Sebastian Bonhoeffer,[3] and Markus G. Manz[1,2]

[1]Institute for Research in Biomedicine, CH-6500 Bellinzona, Switzerland
[2]Division of Hematology, University Hospital Zürich, CH-8091 Zürich, Switzerland
[3]Institute of Integrative Biology, ETH Zürich, CH-8092 Zürich, Switzerland

Hematopoietic stem cells (HSCs) maintain blood production. How often mouse HSCs divide and whether each HSC contributes simultaneously, sequentially, or repetitively to hematopoiesis remains to be determined. We track division of 5-(and-6)-carboxyfluorescein diacetate succinimidyl ester (CFSE)–labeled HSC in vivo. We found that, in steady-state mice, bone marrow cells capable of reconstituting lifelong hematopoiesis are found within both fast-cycling (undergoing five or more divisions in 7 wk) and quiescent (undergoing zero divisions in 12–14 wk) lineage marker–negative c-Kit$^+$ Sca-1$^+$ populations. The contribution of each population to hematopoiesis can fluctuate with time, and cells with extensive proliferative history are prone to return to quiescence. Furthermore, injection of the bacterial component lipopolysaccharide increased the proliferation and self-renewal capacity of HSCs. These findings suggest a model in which all HSCs undergo dynamic and demand-adapted entry into and exit out of the cell cycle over time. This may facilitate a similar degree of turnover of the entire HSC pool at the end of life.

CORRESPONDENCE
Markus G. Manz:
Markus.Manz@usz.ch

Abbreviations used: APC, allophycocyanin; Flt3, Fms-like tyrosine kinase 3; H2B-GFP, histon 2B GFP; HSC, hematopoietic stem cell; LK, Lin$^-$c-Kit$^+$Sca-1$^-$; LKS, Lin$^-$c-kit$^+$Sca-1$^+$; PB, peripheral blood; TLR, Toll-like receptor.

BM is one of most actively proliferating tissues of the body. In humans, ~10^{11}–10^{12} mature blood cells are generated per day (Gordon et al., 2002) from short-lived highly proliferative hematopoietic progenitors which arise from a rare population of hematopoietic stem cells (HSCs) with multilineage differentiation and self-renewal capacity (Kondo et al., 2003). Transplantation studies in mice have shown that a single HSC is capable of reconstituting and maintaining all hematopoietic lineages in lethally irradiated recipients for their respective lifetime (Osawa et al., 1996a; Kiel et al., 2005), or even longer in assays of serial transplantation (Harrison and Astle, 1982; Allsopp et al., 2003); however, physiological hematopoiesis is at least oligoclonal at any given time, indicating that it is not maintained by offspring of one single HSC (Jordan and Lemischka, 1990; McKenzie et al., 2006). Adult BM provides a specialized microenvironment for HSCs, the so-called "niche," that allows HSC maintenance at homeostatic levels. This process is controlled by both intrinsic and extrinsic signals, as demonstrated in multiple animal models with genetic alterations in nonhematopoietic and hematopoietic tissues (Orford and Scadden, 2008).

Steady-state HSC cycling kinetics have been evaluated by in vivo labeling assays with BrdU (Cheshier et al., 1999; Kiel et al., 2007) and biotin (Nygren and Bryder, 2008) and, in recent studies, using both BrdU labeling and histone 2B GFP (H2B-GFP) transgenic mouse models (Wilson et al., 2008; Foudi et al., 2009). BrdU and biotin labeling suggested that all HSCs divide, on average, every 17.8 d, whereas combined BrdU and H2B-GFP experiments revealed two HSC populations, one actively dividing about every 9–36 d and one dividing approximately every 56–145 d (Wilson et al., 2008; Foudi et al., 2009). Assuming conserved division rates in these populations in steady state during a 2-yr laboratory mouse lifetime, the former experiments suggest that HSCs divide ~42×, whereas the latter suggest that one population would divide ~20 times and the other 5 times. This might imply that slow dividing

H. Takizawa and R.R. Regoes contributed equally to this paper.

The Rockefeller University Press $30.00
J. Exp. Med. Vol. 208 No. 2 273-284
www.jem.org/cgi/doi/10.1084/jem.20101643

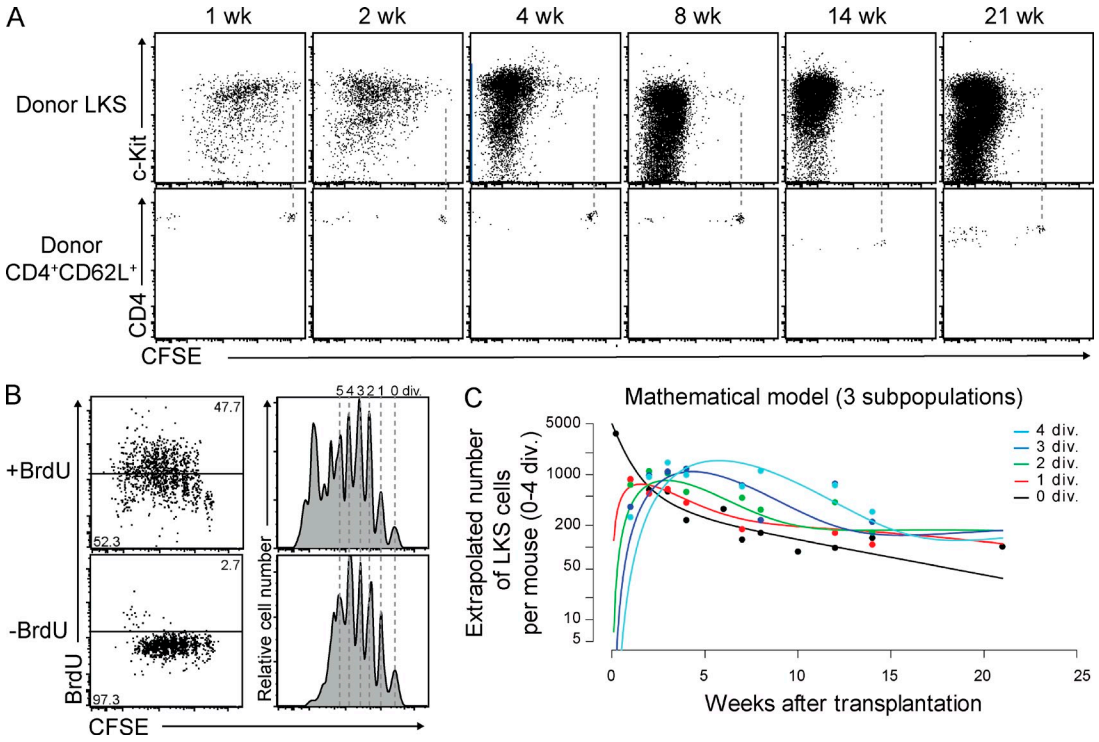

Figure 1. Steady-state divisional heterogeneity of LKS cells revealed by in vivo CFSE dilution. (A) Representative dot plots of BM gated on donor CD45+Lin− (top) and spleen gated on donor CD45+ CD4+CD62L+ (bottom) cells at the indicated time points after transplantation of CFSE-labeled LKS cells and CD4+CD62L+ cells into nonirradiated mice, respectively. Dashed lines represent CFSE intensity of CD4+CD62L+ cells indicating zero division. (B) Comparison of in vivo CFSE dilution and BrdU labeling. Dot plots and histograms show representative CFSE-labeled donor LKS cells 3 wk after transplantation and after 2 wk of in vivo BrdU labeling and control, respectively. Dashed lines illustrate single divisions. (C) Mathematical model of three LKS subpopulations fitting the CFSE labeling data. See also Materials and methods.

HSCs would not contribute to relevant amounts of mature blood cells and could be a dormant reserve, only recruited upon hematopoietic challenge (Wilson et al., 2008; Foudi et al., 2009). However, the faster cycling HSCs repopulated lethally irradiated animals only in the short term, whereas the dormant HSCs showed long-term repopulation (Wilson et al., 2008; Foudi et al., 2009). Therefore, these findings face difficulty in explaining how high-throughput hematopoiesis is maintained by only a small HSC fraction with long-term potential but a very slow division rate. An alternative explanation would be that a single steady-state HSC pool exists that contains stochastically changing slow and fast dividing HSCs, with most HSCs within the pool dividing longitudinally at similar rates.

Although in steady-state adult mice more than two-thirds of HSCs are in a resting, i.e., G0/G1 phase of cell cycle (Cheshier et al., 1999), HSC division can be induced in situations of hematopoietic challenge, for example, chemotherapeutic treatment, irradiation, and BM transplantation (Trumpp et al., 2010). Recently, it was demonstrated that HSC-enriched populations express Toll-like receptors (TLRs), which recognize bacterial or viral molecules, and that TLR ligation causes proliferation and enhances production of innate immune cells such as macrophages and dendritic cells for respective host defense (Nagai et al., 2006; Massberg et al., 2007). Also, some cytokines produced by immune cells in response to viral or bacterial infection can activate quiescent HSC (Essers et al., 2009; Sato et al., 2009; Baldridge et al., 2010). However, it is thus far unclear if these naturally occurring stimulants trigger only differentiation or also accelerated HSC self-renewal. To address the questions of how often HSCs divide and, thus, possibly contribute simultaneously, sequentially, or repetitively to steady-state hematopoiesis, of whether there is a relationship between divisional history and blood forming or repopulating ability, and if HSC self-renewal is increased in hematopoietic stress upon severe infectious challenge, we set up an in vivo HSC divisional tracking system using CFSE labeling.

RESULTS

In vivo CFSE dilution reveals steady-state divisional heterogeneity of Lin−c-kit+Sca-1+ (LKS) cells

Because ∼1% of HSCs are estimated to circulate in steady-state blood, and some of them physiologically rehome into the ∼1% unoccupied BM HSC niches (Wright et al., 2001; Bhattacharya et al., 2006, 2009), we reasoned that i.v. transfer of HSC into nonirradiated mice resembles this process competitively and thus allows evaluation of steady-state HSC divisional dynamics. To track HSC division with high resolution, we labeled cells with CFSE, a fluorescent dye which is

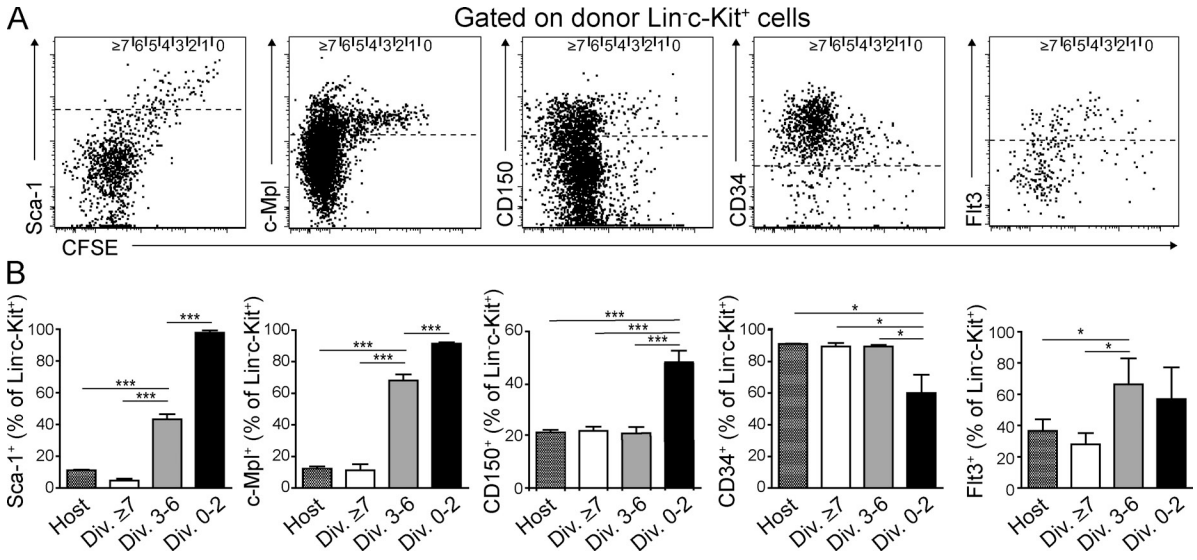

Figure 2. Expression of HSC surface markers upon division of CFSE-labeled LKS cells in BM. (A) Representative dot plots gated on BM donor Lin$^-$c-Kit$^+$ cells depicting CFSE label versus Sca-1, c-Mpl, CD150, CD34, and Flt3 expression 3 wk after transplantation of 10^5 CFSE-labeled LKS cells into nonirradiated recipients. Dashed lines represent cutoff regarded as positive. 0 to ≥7 divisions (indicated at top of dot plots) were determined according to CFSE intensity. (B) Percentage of Lin$^-$c-Kit$^+$ cells, positive for indicated surface antigens within total host or 0–2×-, 3–6×-, and ≥7×-divided donor populations (shown in A). Mean ± SD is shown (n = 4–6 from three to six independent experiments for each stain). *, $P < 0.05$; ***, $P < 0.001$.

equally distributed to daughter cells upon each cellular division (Weston and Parish, 1990; Lyons and Parish, 1994). CFSE labeling did not impair HSC function, as CFSE-labeled LKS cells containing HSCs successfully engrafted nonirradiated animals with stable chimerism of ∼1% over at least 20 wk (unpublished data). Transplantation of 10^5 LKS into nonirradiated mice revealed that 0×-divided Lin$^-$c-Kit$^+$ cells with an equivalent CFSE intensity to that of naive CD4$^+$CD62L$^+$ T cells transferred to determine zero cell division CFSE intensity. When mice were irradiated before LKS transfer, all donor-derived LKS cells had divided ≥5× in 3 wk and high BM and blood chimerism was established as expected (Fig. S1). Weekly BM analysis of nonirradiated recipient mice transplanted with CFSE-labeled LKS showed that most of the donor cells divided within 4 wk, whereas a small fraction did not divide over 21 wk, the longest period observed (Fig. 1 A). 0×-divided cells were maintained in the BM, but not in the spleen, and included LKS cells with a CD150$^+$ and CD34$^-$ phenotype, which are reported to be highly enriched for quiescent HSC (Osawa et al., 1996a; Kiel et al., 2005; Fig. S2, A and B). These data demonstrate that in steady state the majority of LKS cells divide actively and a small fraction is quiescent.

To compare the HSC-tracking method established in this study with BrdU labeling (Cheshier et al., 1999; Kiel et al., 2007), mice were treated with BrdU starting 1 wk after CFSE-labeled LKS cell transfer. BrdU treatment led to more LKS divisions, confirming a mitogenic effect of BrdU (Kiel et al., 2007; Wilson et al., 2008; Fig. 1 B). However, BrdU incorporation neither correlated linearly with divisions nor allowed divisional resolution. Most importantly, BrdU did not recruit all LKS cells into division, leaving behind a fraction of 0×-divided non–BrdU-labeled LKS. These data demonstrate that CFSE labeling provides high-resolution single-division HSC tracking and reveal that BrdU labeling alters cell cycle kinetics but, as expected, does not mark the remaining quiescent cells. This fact might have had a profound impact on readout and interpretation of previous studies using the BrdU labeling and chase assay to evaluate HSC turnover, as cells are recruited into division and only recently divided and labeled cells are subsequently monitored, and most 0×-divided quiescent cells are not included in the chased population (Cheshier et al., 1999; Wilson et al., 2008).

To estimate the turnover and loss rate of total LKS cells, i.e., a population which contains but is not exclusively composed of HSCs (Osawa et al., 1996b), we developed mathematical models assuming that the LKS cell population is composed of one, two, three, or four subpopulations with differing rates of proliferation and loss. Fitting these mathematical models to the CFSE dilution data revealed at least three subpopulations with different division and differentiation kinetics (see Materials and methods and Table S1). One population was characterized by a high rate of loss and no proliferation, and the remaining two populations roughly correspond to the fast-cycling and dormant populations identified previously (Wilson et al., 2008; Foudi et al., 2009).

Expression of HSC and lineage-differentiation markers by LKS cells upon division

To correlate divisional history with HSC and progenitor cell–associated surface marker expression, we analyzed lineage negative cells in BM 3 wk after transfer. 0–2×-divided donor Lin$^-$c-kit$^+$ cells were positive for Sca-1 (>98%) and the thrombopoietin receptor c-Mpl (>93%), both of which are

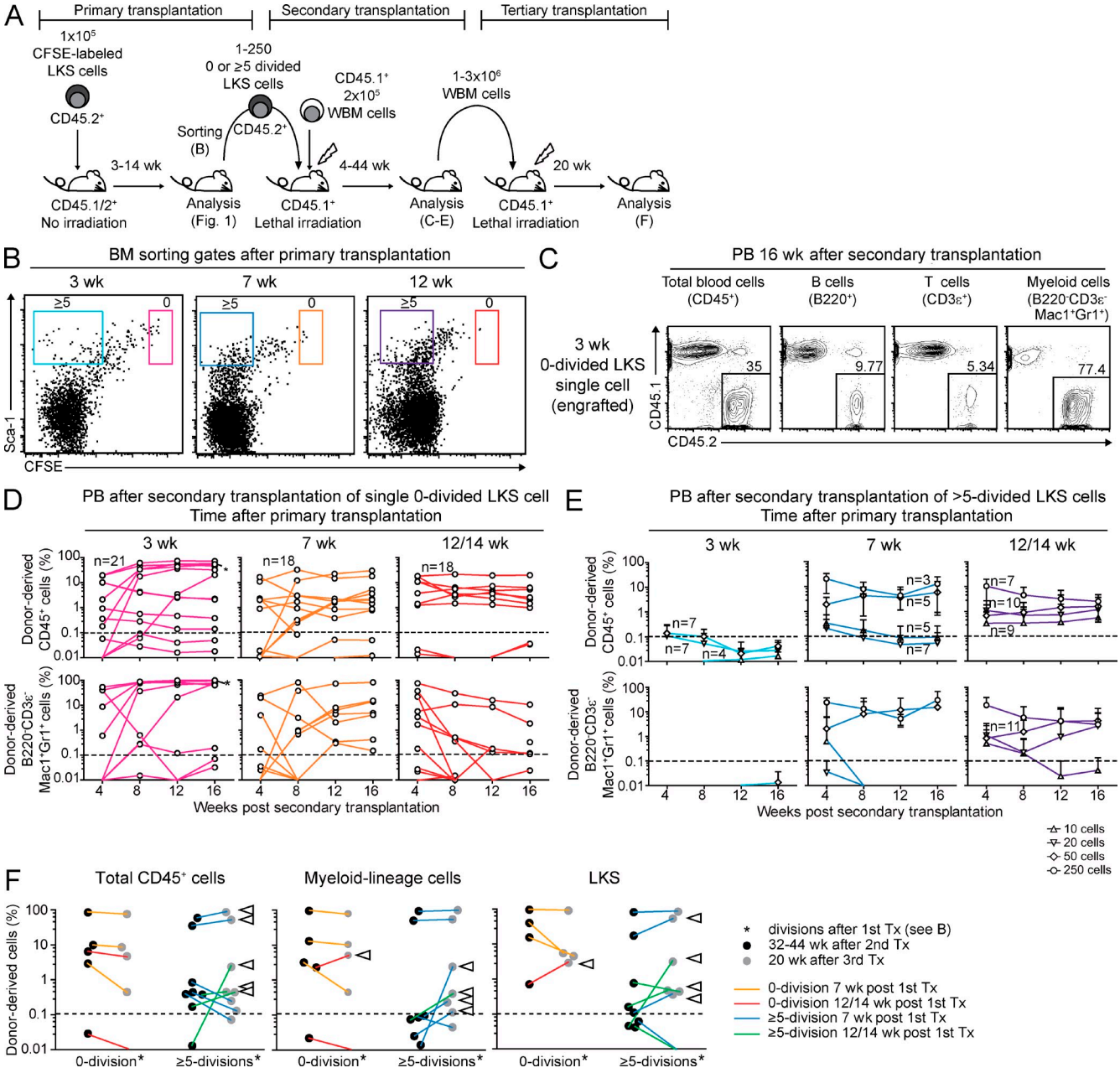

Figure 3. HSCs have heterogeneous divisional activity. (A) Experimental scheme of sequential transplantation. (B) Representative dot plots of BM from primary LKS transplant recipients gated on donor Lin⁻c-Kit⁺ cells. Sorting gate for 0×- (red, orange, and pink) and ≥5×-divided LKS cells (light blue, dark blue, and purple) are shown at the indicated time points after primary transplantation. (C–E) PB donor chimerism in indicated populations after secondary transplantation with single 0×-divided LKS cells (C and D) or 10–250 ≥5×-divided LKS cells (E). (C) Representative PB FACS dot plots 16 wk after secondary transplantation with a single 0×-divided LKS cell sorted from primary recipients at 3 wk after LKS transfer. (D) Each line represents sequential data from individual animals (n = 18–21 mice as indicated from four to five independent experiments). Asterisk shows engraftment data of the animal shown in C. Range of donor CD45⁺ chimerism in engrafted mice 4 mo after secondary transplantation: 32.7–72%, 1.8–22.5%, and 1.0–19.9% in mice transplanted with LKS cells isolated 3, 7, and 12/14 wk after primary transplantation, respectively. (E) Lines represent all data from four independent experiments with SD error bars (number of mice in each group are indicated at each line). (F) Long-term engraftment of 0×- or ≥5×-divided LKS cells in secondary and tertiary transplants. Donor chimerism in total CD45⁺ cells, myeloid cells, and LKS cells in BM was examined 32–44 wk after secondary transplantation (black dots) and 20 wk after tertiary transplantation (gray dots). Each connecting line shows data derived from identical primary donor cells. Arrows represent increase in contribution to hematopoiesis after tertiary transplantation. Dashed line at 0.1% marks cut off determined for nonengraftment.

Table I. Transplantation of 0×-, 0–2×-, or ≥5×-divided LKS cell into lethally irradiated mice reveals steady-state cycling heterogeneity in HSC

Cells injected	Cell dose	Secondary recipient mice with long-term multilineage reconstitution		
		Sorting time points after primary transplantation		
		Week 3	Week 7	Week 12/14
0×-divided	1	24 (5/21)	22 (4/18)	28 (5/18)
0–2×-divided	10	67 (4/6)	100 (5/5)	ND
0–2×-divided	20	100 (7/7)	ND	ND
≥5×-divided	10	0 (0/4)	0 (0/5)	11 (1/9)
≥5×-divided	20	0 (0/7)	0 (0/7)	10 (1/10)
≥5×-divided	50	0 (0/7)	20 (1/5)	36 (4/11)
≥5×-divided	250	ND	67 (2/3)	71 (5/7)

The indicated numbers of LKS cells at the indicated time points after primary transplantation were deposited into individual wells of 96-well plates. The contents of each well were injected into lethally irradiated animals along with 2×10^5 total BM cells. After 4 mo, PB of transplanted mice was analyzed on flow cytometry to identify mice that were multilineage reconstituted by donor cells (above background: >0.1% in $B220^+$, $CD3\varepsilon^+$, and $B220^-CD3\varepsilon^-CD11b^+Gr\text{-}1^+$ cells). The numbers in the time point columns represent the percentage of engrafted mice, and the parenthetical numbers represent the number of engrafted mice per number of transplanted mice. ND, not determined.

highly expressed in HSC (Spangrude et al., 1988; Qian et al., 2007; Yoshihara et al., 2007), and their expression decreased with division. 40–50% of 0–2×-divided cells were positive for CD150 (Kiel et al., 2007) and negative for CD34 (Osawa et al., 1996a), and Fms-like tyrosine kinase 3 (Flt3) expression (Christensen and Weissman, 2001; Karsunky et al., 2003) was low in 0–2×-divided and up-regulated in 3–6×-divided cells (Fig. 2). Some $Lin^-c\text{-}Kit^+$ cells started to express markers of lineage commitment like M-CSFR (Onai et al., 2007), IL-7Rα (Kondo et al., 1997), and FcγRII/III (Akashi et al., 2000; Kondo et al., 2003) after more than three divisions (Fig. S2, C and D). Thus, surface marker expression pattern analysis demonstrates that at 3 wk after transfer, 0–2×-divided cells displayed a HSC immunophenotype. Furthermore, LKS cell differentiation to lymphoid or myeloid lineage-committed progenitors required at least three divisions in steady state.

Heterogeneous cycling activity of functional HSCs

As HSCs represent a minority within LKS cells (Osawa et al., 1996b) and LKS cell division does not necessarily reflect HSC divisional dynamics, we determined HSC frequency by in vivo single-cell and limiting dilution repopulation and serial transplantation assays. We reisolated defined numbers of donor LKS cells based on their divisional history at different time points after primary transfer (Fig. 3 B) and transplanted these into lethally irradiated secondary recipient mice along with irradiation-protective whole BM cells, followed by monthly analysis for donor engraftment (Fig. 3 A). Transplantation of single 0×-divided LKS cells, isolated 3–14 wk after primary transplantation, yielded multilineage reconstitution in 22–28% of irradiated mice for 16 wk (Fig. 3, C and D; Table I; and Fig. S3). Up to 250 LKS cells that had divided ≥5× in 3 wk in primary recipients showed no engraftment, whereas 50–250 ≥5×-divided LKS cells at 7 or 12–14 wk after primary transfer contained long-term multilineage repopulating HSCs (Fig. 3 E, Table I, and Fig. S3). Based on in vivo limiting dilution transplantation, the frequency of HSC in ≥5×-divided LKS cells at 7 and 12–14 wk was 1:293 and 1:153, respectively (Fig. S3 D). BM LKS $CD34^-$ cell analysis revealed maintenance of donor chimerism within this HSC-enriched cell fraction over 6 mo (Fig. S4).

We next tested serial long-term hematopoietic potential of 0×- and ≥5×-divided LKS cells by transferring whole BM cells from engrafted secondary recipients into lethally irradiated tertiary recipient mice (Fig. 3 A). Both 0×- and ≥5×-divided LKS cells were able to reconstitute BM compartments of irradiated mice for a total of 52–64 wk, i.e., >1 yr, over serial transplantation. Donor chimerism varied depending on individual mice but not on divisional history of donor cells from primary transplants (Fig. 3 F). Given that nonconditioned i.v. transfer reflects steady-state physiological HSC circulation and BM rehoming (Wright et al., 2001; Bhattacharya et al., 2006; Méndez-Ferrer et al., 2008), these findings, in contrast to previous studies (Wilson et al., 2008; Foudi et al., 2009), directly demonstrate cycling heterogeneity in steady-state HSC; some HSCs are quiescent over months and consequently do not contribute to blood production, whereas others possess high cycling activity and, thus, likely contribute to blood cell production during this time.

To determine the mean turnover rate of HSC, we calculated the number of HSC in division classes 0 and ≥5 from the repopulation assay data (Fig. 4 A and Table S2) and fitted a mathematical model to the number of HSC, assuming that their division rate is equal to the rate of loss, and, hence, the total HSC number in this steady-state model is constant over time (see Materials and methods). We estimate that HSCs divide, on average, every 39 d (95% confidence interval 20–50 d), leading to a total of ∼18 divisions during a lifetime of a mouse. As there was no statistical evidence for heterogeneous division rates in the functional biologically defined HSC population, this indicates that HSCs with long-term reconstitution capacity are not necessarily permanently split into subpopulations with different cycling kinetics (Wilson et al., 2008; Foudi et al., 2009).

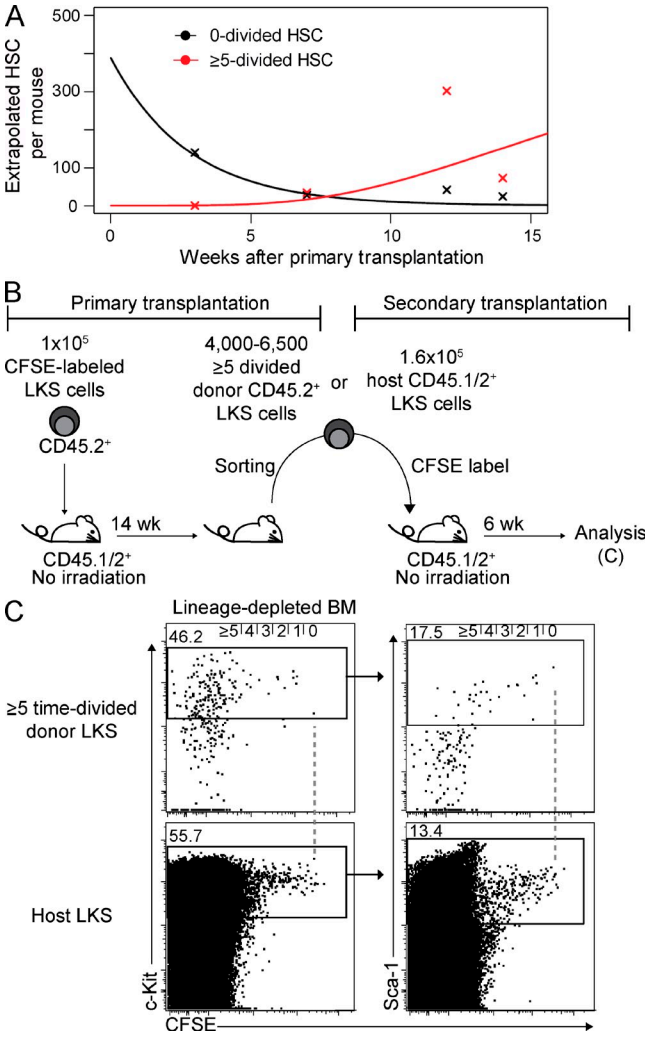

Figure 4. Maintenance of biologically defined HSCs over time and steady-state serial transplantation revealing changing divisional frequencies of LKS. (A) Mathematically calculated mean number of 0×- or ≥5×-divided biologically defined HSCs per mouse over time based on engraftment data described in Materials and methods and Table S2. (B) Experimental scheme of steady-state serial transplantation of cycling LKS cells into nonirradiated mice. (C) Representative dot plots of BM from secondary transplants gated on donor (CD45.2+) or host (CD45.1/2+) Lin− cells at 6 wk after secondary transplantation. Dashed lines represent zero division.

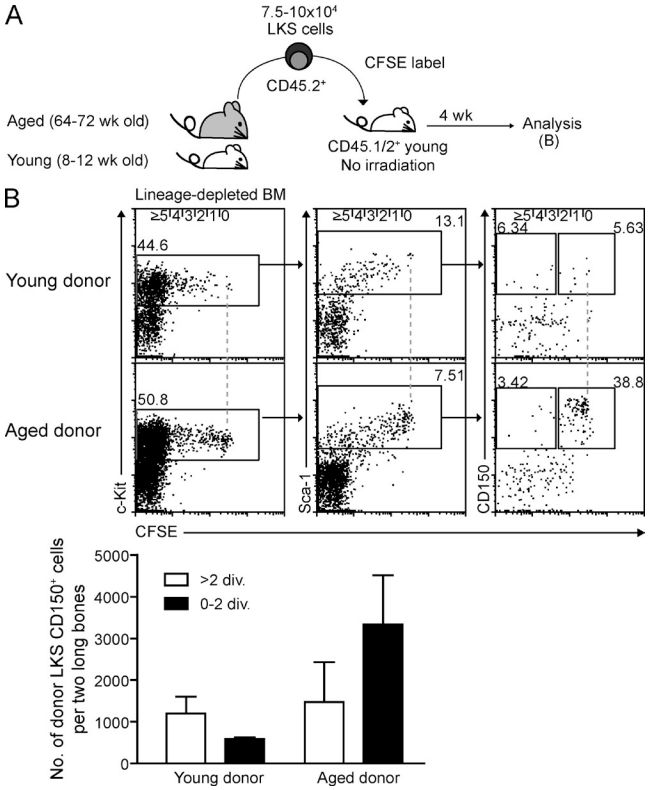

Figure 5. Increased dormancy of LKS CD150+ cells associated with steady-state aging. (A) Experimental scheme of transplantation. Young mice were transplanted with 7.5–10 × 10^4 CFSE-labeled LKS cells from young (8–12 wk old) or aged (64–72 wk old) mice and analyzed after 4 wk. (B) Representative dot plot analysis of lineage-depleted BM gated on donor Lin− cells. Dashed lines represent zero division. Number of donor LKS CD150+ cells having undergone indicated numbers of divisions were calculated. Graph shows mean ± SD (n = 3 mice from two to three independent experiments).

Changing divisional frequencies of LKS cells revealed by steady-state serial transplantation

Virus-mediated HSC marking suggested that hematopoiesis is maintained by stem cell clones that asynchronously self-renew and differentiate (Lemischka et al., 1986; McKenzie et al., 2006). Consistent with those findings, our serial transplantation experiments showed that the donor contribution to mature blood cells and LKS cells varied and increased in some tertiary recipients (Fig. 3 F, arrowheads). Secondary and tertiary recipients contained blood-forming cells derived from single 0×-divided HSCs and, according to limiting dilution transplantation experiments, single or double ≥5×-divided HSCs. Thus, the fluctuating hematopoietic contribution indicates that some HSC clones or their offspring vary in contribution to blood production over time. This is consistent with recent publications indicating reactivation of HSCs from quiescence over time (Morita et al., 2010).

To address the question of whether divisional frequency is kept constant or if steady-state fast-dividing LKS cells naturally vary turnover rates, we performed steady-state serial transplantation with fast-cycling cells. 4,000–6,500 LKS cells that had divided ≥5× at 14 wk after primary transplantation were reisolated, labeled again with CFSE, and subsequently transplanted into secondary nonirradiated animals (Fig. 4 B). Assuming constant divisional frequency, transferred cells should divide at least ≥2× within 6 wk. However, some donor LKS cells remained in the zero- or onefold division, demonstrating that fast-cycling cells or their progeny can slow down the divisional rate in steady state (Fig. 4 C).

Increased dormancy of aged LKS CD150+ and expanded LKS cells

Next, we examined whether steady-state aging or massive hematopoietic system expansion after lethal irradiation and BM

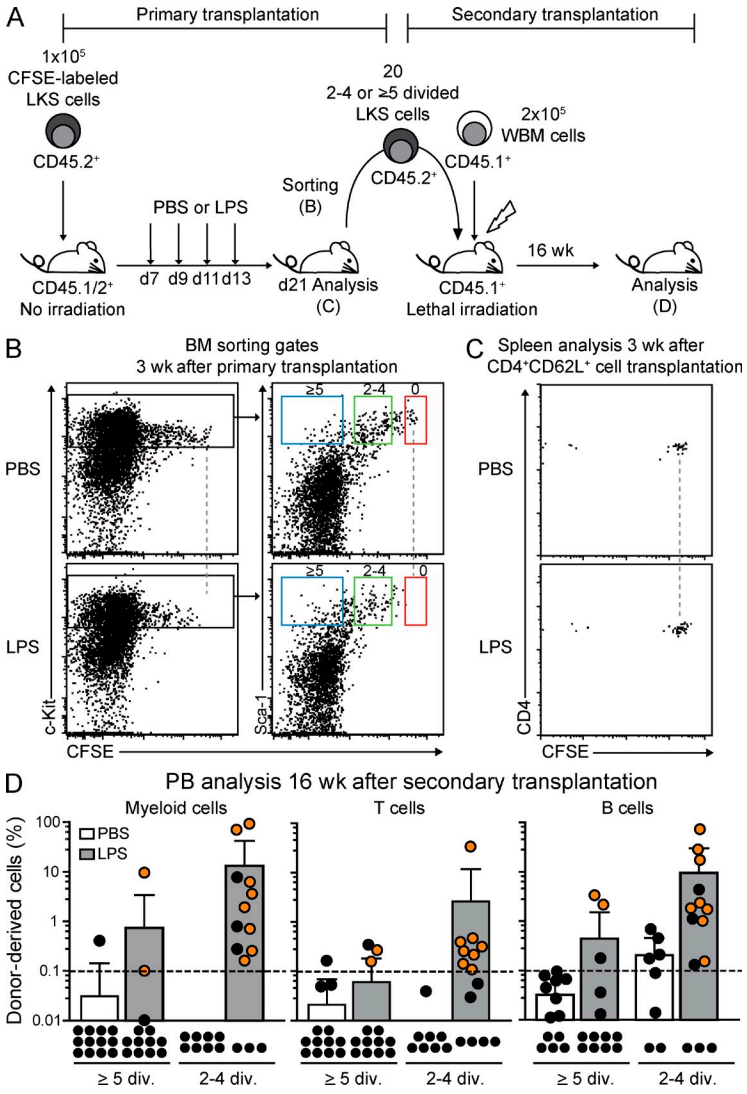

Figure 6. In vivo LPS challenge recruits HSCs into division. (A) Experimental scheme of transplantation and LPS challenge. (B) Representative dot plots gated on donor Lin⁻ cells from BM of primary transplant recipients at day 21 after transfer of CFSE-labeled LKS cells with or without four injections of LPS. Sorting gates for 0×- (red), 2–4×- (green), or ≥5×-divided LKS cells (blue) are shown. Dashed lines represent zero division. (C) Representative dot plots gated on donor CD4⁺CD62L⁺ cells from spleen of primary transplant recipients at day 21 after transfer of CD4⁺CD62L⁺ cells with or without four injections of LPS . Dashed lines represent zero division. (D) PB donor engraftment within myeloid, T, and B cells 4 mo after secondary transplantation with 20 2–4×- or ≥5×-divided LKS cells from PBS- or LPS-treated mice (B). Pooled data from three independent experiments are shown as dots (representing one mouse each) and a bar graph depicting mean ± SD. Orange dots show the multilineage reconstituted animals. Black dots show animals with one or zero lineages reconstituted. The dashed line at 0.1% shows background threshold set for engraftment cutoff. ND, not detected.

transplantation with low HSC numbers, i.e., both states with overall increased HSC divisional history, affects cell cycle kinetics of HSC-enriched cells. CFSE-labeled LKS cells from aged and young mice were transplanted into steady-state young mice. The frequency and number of 0×-dividing or slow-dividing LKS CD150⁺ was substantially increased in mice transplanted with aged cells (Fig. 5, A and B). Similarly, CFSE-labeled LKS cells from mice that were transplanted 16 wk previously with low numbers of HSCs showed an increased ratio of slow-dividing and quiescent to fast-dividing cells (unpublished data). This data demonstrates that LKS cells, containing HSCs with an increased divisional history, have a tendency to return to quiescence. If this reflects a general biological feature of HSCs, steady-state fast-dividing HSCs will slow down their divisional rate, once given the opportunity in a permissive environment.

Recruitment of HSC into division upon in vivo LPS challenge

Immunophenotypically defined HSCs have been shown to recognize viral or bacterial components through TLRs and, subsequently, undergo division at peripheral sites to give rise to innate immune cells (Nagai et al., 2006; Massberg et al., 2007). However, there is no direct evidence that quiescent HSCs in BM increase division and self-renewal to contribute to blood cell production upon demand in vivo. We tested if LPS challenge, as a surrogate for gram-negative infection which induces massive myeloid cell production, would recruit quiescent HSCs into cycle. Mice that had been previously transplanted with CFSE-labeled LKS cells were repetitively treated with LPS and analyzed 8 d after final LPS injection (Fig. 6 A). Although 0×-divided control T cells were detectable, 0×-divided LSK cells were absent, and the number of ≥5×-divided LKS cells was increased in LPS-treated mice (Fig. 6, B and C), indicating cell loss or recruitment of LKS cells into cell cycle. To evaluate HSC potential in 2–4×- or ≥5×-divided LKS cells from PBS- or LPS-treated mice, cells were reisolated and transplanted into lethally irradiated secondary recipients (Fig. 6 A). 4 mo after transplantation, donor chimerism in peripheral blood (PB) and contribution to different lineage cells were examined. Consistent with previous experiments (Fig. 3 E), donor cell engraftment was rarely detected in secondary recipients transplanted with 2–4×- and ≥5×-divided LKS cells from PBS-injected control mice. In marked contrast, both 2–4×- and ≥5×-divided LKS cells from LPS-injected mice contributed to the generation of multilineage hematopoiesis in more than half and in some of the recipients, respectively, after 16 wk (Fig. 6 D). Lineage distribution analysis in secondary transplanted animals showed no lineage-biased repopulation, indicating that LPS challenge does not affect cell fate or differentiation potential of HSC (unpublished data). Thus, this data provides the first evidence that a naturally occurring hematoimmunological challenge, such as gram-negative bacterial infection, induces

proliferation and self-renewal of HSCs, a mechanism which might have evolved to enhance fitness to rapidly amplify innate immune responses upon demand.

DISCUSSION

Using a newly established HSC tracking method that utilizes in vivo CFSE dilution, we communicate three major findings on HSC turnover and contribution to blood formation in steady state and upon inflammation. The first finding is that in steady state, HSCs with equivalent life-long multilineage repopulation potential are contained in both frequently cycling cell populations that divide ≥5× in 7 wk, i.e., about every 1.4 wk, and in quiescent cells that do not divide over 14 wk. The finding is not consistent with the previous observations that only quiescent cells possess serial reconstitution capacity and fast-diving cells have limited self-renewal (Wilson et al., 2008; Foudi et al., 2009). This contradiction might arise from technical issues, as numbers of cells transferred into secondary transplants, and from sensitivity and resolution of divisional tracking methods. Another possibility would be that the dividing HSCs are not included in the population with LKS $CD48^{-}CD150^{+}$ phenotype as subsets of HSC might not express CD150 (Weksberg et al., 2008). Although it was assumed that both BrdU incorporation and H2B-GFP transgenic animal models allow us to follow seven cellular divisions, our comparative analysis demonstrates that staining intensity for BrdU detection reaches a limit at two to three divisions and that BrdU staining is not linear, suggesting a lower divisional resolution of BrdU retention than expected, whereas, in contrast, CFSE dilution can distinguish at least five divisions with high resolution. Furthermore, the fact that BrdU has mitogenic activity, which has been shown in this paper and previously (Kiel et al., 2007; Wilson et al., 2008), has a substantial impact on the experimental readout because BrdU labeling changes cell cycle state as well as, potentially, consecutive function of cells. Also, most quiescent 0×-dividing HSCs are ignored in the BrdU assay, as our data shows remaining CFSE-high cells that do not incorporate BrdU. Thus, with some HSCs being deeply quiescent and inactive in DNA replication and protein synthesis, uniform labeling of all HSC by DNA labeling or marker protein expression might not be achieved at the starting point of chase. This contrasts with the CFSE labeling established in this paper that ensures highly uniform labeling and high-resolution divisional tracking of cells without impairing HSC function, independent of cell cycle activity during the labeling process.

The second finding is that steady-state fast-cycling populations can slow down over time in steady-state serial transplantation and that LKS $CD150^{+}$ cells containing HSCs with extensive proliferative history—i.e., HSCs that have gone through extended proliferation in aging or after in vivo challenge by transplantation—are prone to return to quiescence. As demonstrated in this paper, divisional activity is not associated with HSC function in young adult mice. Furthermore, HSCs have the capacity to engraft and constitute long-term hematopoiesis over several serial transplantations, indicating that high divisional history does not lead to immediate loss of HSC function (Allsopp et al., 2001). HSC cycling activity is a result of extrinsic and intrinsic regulation (Orford and Scadden, 2008). Based on our data, we would like to suggest that steady-state fast-cycling or enhanced turnover with aging or irradiation- and transplantation-induced proliferation might activate an intrinsic HSC program that, based on divisional history, drives toward quiescence. Thus, an intrinsic cell memory effect to prevent HSC exhaustion might be counterbalanced by an extrinsic drive for proliferation. The underlying mechanisms will need to be determined in the context of environmental cues such as availability of adhesion molecules and growths factors in the putative BM HSC niche.

Third, we show that in vivo TLR4 agonist challenge recruits in vivo functional quiescent HSCs into proliferation and self-renewal with nonbiased lineage repopulation capacity. Although TLR ligation on HSCs has been shown to induce cellular division and myeloid lineage-skewed differentiation ex vivo, there was no direct evidence for enhanced self-renewal of HSC in BM (Nagai et al., 2006; Massberg et al., 2007). It is not clear from our experiments if LPS executes its effect on cell cycle regulation directly via TLR4 expressed on HSCs, via an indirect pathway, or via a combination of both. Hematopoietic and nonhematopoietic cell–secreted interferons have been recently identified by several studies to drive HSC in cycle upon artificial addition or in chronic infection (Essers et al., 2009; Sato et al., 2009; Baldridge et al., 2010). Our study extends these findings and directly demonstrates that correlates of gram-negative infections, or possibly self-damage (Rakoff-Nahoum and Medzhitov, 2009), can signal from the periphery to primary hematopoietic sites in BM and have an impact on divisional behavior of HSCs. This mechanism likely allows adequate hematopoietic responses and, at the same time, prevents loss of HSCs by differentiation.

Our mathematical simulation reveals that HSCs with different cycling activity can be contained in one HSC population with relatively broad cycling variation and that, on average, HSCs divide 18× during a 2-yr lifespan of a laboratory mouse. Two principle models have been posed for the maintenance of hematopoiesis by stem cells. The clonal maintenance model suggests that all HSCs give rise to mature blood cells continuously throughout life and, thus, all HSCs should divide similarly to produce cells that contribute to blood formation (Fig. S5 A; Jordan and Lemischka, 1990; Cheshier et al., 1999; McKenzie et al., 2006; Kiel et al., 2007; Nygren and Bryder, 2008). The clonal succession model proposes that some HSCs divide frequently, contribute to hematopoiesis, and fully differentiate or die subsequently and are followed by previously quiescent HSCs that then meet the same fate (Fig. S5 B; Kay, 1965; Drize et al., 1996; Wilson et al., 2008; Foudi et al., 2009). Based on our data, we suggest a "dynamic repetition" model, where some HSCs dominate blood formation for a time, subsequently enter a quiescent state in which other HSCs increase hematopoietic contribution, and get reactivated again and contribute to blood formation in repetitive cycles (Fig. S5 C). Our data do not suggest how long active and resting phases might last or how many

HSC clones at any given time contribute to hematopoiesis. However, the model of steady-state reversible change between proliferation and quiescence in HSCs over time is consistent with virtual single cell–based simulation models (Glauche et al., 2009). Furthermore, the dynamically changing cycling activity likely results in a similar turnover of the entire HSC pool, indicating a homogeneous divisional history for all HSCs at the end of life, a suggestion which would be coherent with linear telomere shortening observed in the human aging HSC pool (Rufer et al., 1999). The findings reported in this paper might represent a biological principle that could hold true for other somatic stem cell–sustained organ systems and might have developed during evolution to ensure equal distribution of work load, efficient recruitment of stem cells during demand, and reduction of risk to acquire genetic alterations by alternating fractions of stem cells in quiescence at any given time.

MATERIALS AND METHODS

Mice. C57BL/Ka-Thy1.1 (CD45.1$^+$ or CD45.2$^+$) mice were bred and maintained at the Institute for Research in Biomedicine animal facility. CD45.1/2$^+$ F1 mice were generated by crossbreeding. 8–12-wk-old or 64–72-wk-old mice were used in the studies. Mice were treated in accordance with the guidelines of the Swiss Federal Veterinary Office, and experiments were approved by the Dipartimento della Sanità e Socialità and Gesundheitsdirektion Kanton Zürich, Veterinäramt.

Cell isolation and sorting. Total BM cells were harvested from long bones, red blood cells were lysed with ACK lysis buffer (150 mM NH_4Cl, 10 mM $KHCO_3$, and 0.1 mM EDTA), and debris was removed with 70-µm cell strainers (BD). Cells were stained with PE-Cy5–conjugated antibodies against the lineage antigens B220 (RA3-6B2), CD3ε (145-2C11), Ter119 (Ter119), and Gr-1 (RB6-8C5) and immunomagnetically enriched for lineage-negative cells using anti-Cy5/anti–Alexa Fluor 647 Microbeads (Miltenyi Biotec). The lineage-depleted cells were subsequently stained with allophycocyanin (APC)-Cy7–conjugated antibody to c-Kit (2B8) and FITC-conjugated antibody to Sca-1 (D7), and LKS or Lin$^-$c-Kit$^+$Sca-1$^-$ (LK) cells were sorted using a FACSAria (BD). Naive CD4$^+$CD62L$^+$ T cells were enriched from spleen cells with PE-Cy5–conjugated anti-CD4 antibody (GK1.5) and anti-Cy5/anti–Alexa Fluor 647 Microbeads, and were then stained with PE-conjugated anti-CD62L antibody (MEL-14) followed by sorting of CD4$^+$CD62L$^+$ cells on a FACSAria. All antibodies were obtained from eBioscience.

CFSE staining and cell transplantation into nonirradiated or sublethally irradiated mice. Sorted cells were labeled for 7 min at 37°C with 2 µM CFSE (Invitrogen) in Dulbecco's PBS (D-PBS; Invitrogen) supplemented with 2% FBS (Invitrogen). The same volume of ice-cold D-PBS with 10% FBS was then added to stop the reaction. After wash with Mg^{2+}/Ca^{2+}-free PBS, 10^5 CFSE-labeled LKS cells (CD45.2$^+$) or 2×10^6 CFSE-labeled CD4$^+$CD62L$^+$ naive T cells (CD45.2$^+$) were i.v. transplanted into nonirradiated recipient F1 (CD45.1/2$^+$) mice. In some cases, mice were sublethally irradiated with 6.5 Gy from a Cesium 137 source (BIOBEAM 8000; STS GmbH) at 3.75 Gy/min before transplantation.

In vivo LPS challenge. 10^5 CFSE-labeled LKS cells were transplanted into nonirradiated animals. 1 wk after transplantation, mice were i.p. injected with PBS or 35 µg LPS from *Escherichia coli* (Ultrapure; InvivoGen) 4×, each with a 2 d-interval, and were analyzed 6 d after the final injection.

Flow cytometric analysis. Lineage-negative cells from BM were enriched from transplanted mice and stained with additional monoclonal antibodies as follows: APC-Cy7–conjugated c-Kit, PE-Cy7-conjugated anti–Sca-1, Pacific blue–conjugated anti-CD45.1 (A20), APC-conjugated anti-CD45.2 (104), PE-conjugated anti-CD150 (TC15-12F12.2; BioLegend), PE-conjugated anti-CD34 (Raw34), PE-conjugated anti-CD16/32 (2.4G2), PE-conjugated IL-7α (A7R34), PE-conjugated anti-Flt3 (A2F10.1), biotinylated anti–c-Mpl (AMM2 donated by Kyowa Hakko Kirin Co., Ltd.), PE-conjugated anti–M-CSFR (AFS98), or PE-Cy5–conjugated antilineage antibody. The biotinylated antibody was detected with PE-conjugated streptavidin. Each single division was determined as follows: a gate for zero division was set on the CFSE peak of the undivided naive T cell control, and subsequent divisions were determined according to reduced fluorescence intensity of peaks in respective histograms. The background fluorescence was determined from nontransplanted BM sample. For evaluation of peripheral engraftment, thymus, spleen, lymph nodes, and PB were harvested and stained with FITC-conjugated anti–Gr-1, PE-conjugated anti-CD11b, PE-Cy5–conjugated CD3ε, APC-Cy7–conjugated B220, PE-Cy7–conjugated CD45.1, and APC-conjugated CD45.2. Before analysis, cells were resuspended in PBS containing 2 µg/ml Hoechst 33342 (Invitrogen). The percentage of donor contribution was assessed by measuring CD45.1$^+$ or CD45.2$^+$ cells in B220$^+$ B-lineage, CD3ε$^+$ T-lineage, or B220$^-$CD3ε$^-$CD11b$^+$Gr-1$^+$ myeloid lineage cells. Cutoff for donor engraftment was determined based on the percentage of nonspecific stain in nontransplanted secondary transplanted recipient. All antibodies were purchased from eBioscience except when otherwise specified.

BrdU retention assay with CFSE labeling. 1 wk after transfer of CFSE-labeled LKS cells into nonirradiated mice, animals were i.p. injected with a single dose of 180 µg BrdU (Sigma-Aldrich) and were fed water containing 800 µg/ml BrdU and 5% glucose for the next 14 d. Mice were then sacrificed and BrdU staining was performed using a BrdU labeling kit (BD). Cells from PBS-treated animals were used as a negative control for BrdU staining.

Single cell and whole BM transplantation into lethally irradiated mice. 3–14 wk after primary transplantation with CFSE-labeled cells, Lin$^-$ cells were immunomagnetically enriched from long bones of mice, as described in Flow cytometric analysis and stained with antibodies to CD45.1, CD45.2, c-Kit, and Sca-1. 1–250 donor-derived LKS cells (CD45.2$^+$) were sorted into individual wells of 96-well plates using a FACSAria. Single cell deposition was confirmed microscopically. 2×10^5 total BM cells from CD45.1$^+$ or CD45.2$^+$ mice were suspended in Mg^{2+}/Ca^{2+}-free Hank's buffered salt solution supplemented with 2% FBS and plated into each well. The content of each well was i.v. injected into mice that were lethally irradiated with 2 × 6.5 Gy in a 4-h interval. Mice were bled monthly, blood was subjected to red blood cell lysis, and donor engraftment was analyzed as described in Flow cytometric analysis. Recipients with >0.1% donor chimerism in B-lineage (B220$^+$), T-lineage (CD3ε$^+$), and myeloid-lineage (B220$^-$CD3ε$^-$CD11b$^+$Gr-1$^+$) population was considered to be multilineage repopulated. The frequency of HSC in LKS cells at the indicated time points after primary transfer was determined according to Poisson statistics (Smith et al., 1991) or L-Calc (STEMCELL Technologies Inc.). For the tertiary transplantation, one to three million cells of total BM cells harvested from secondary transplants were injected into lethally irradiated mice (CD45.1$^+$ or CD45.2$^+$).

Statistical analysis. The significance of differences was determined by an unpaired Student's *t* test.

Mathematical modeling and analysis of LKS cell division kinetics. The simplest model that can be used to describe the division kinetics of CFSE-labeled cells is given by the following differential equations (De Boer et al., 2006):

$$\begin{aligned} dX_0/dt &= -(\lambda + d)X_0 \\ dX_i/dt &= 2\lambda X_{i-1} - (\lambda + d)X_i, \quad i = 1,\ldots,4 \\ dX_{5+}/dt &= 2\lambda(X_4 + X_{5+}) - dX_{5+}. \end{aligned} \tag{1}$$

Here, X_i denotes the number of LKS cells that gave undergone i divisions, and X_{5+} denotes the number of LKS cells that have divided five or more times. The parameter λ is the rate constant for cell division, and d is the rate constant for LKS cell loss. Several processes contribute to this loss of LKS cells. These are differentiation, which leads to a loss of LKS marker, cell death, or loss of LKS marker not related to differentiation. For simplicity, we refer to d as the differentiation rate constant. Because the experiment involved the transfer of 5,000 CFSE-labeled LKS cells into the mice, we assume that at time $t = 0$, all cells are in the division class 0, corresponding to the highest CFSE label, and their number is $X_0(0) = 5{,}000$. (In mathematical immunology, the division of cells is often described by the Smith-Martin model rather than this simple model above [De Boer et al., 2006]. The Smith-Martin model describes the cell cycle in more detail introducing a parameter for the time a cell requires for dividing once it committed to division. However, because the division kinetics of LKS cells is very slow, occurring on the time scale of weeks rather than hours, the time required for cell division can be ignored.)

We constructed extensions of this basic model to study the heterogeneity of the division kinetics of the LKS populations. In particular, we developed versions of the basic model in which we assume two or three subpopulations, each with their own division and differentiation rates. These mathematical models are given by the following set of differential equations:

$$\begin{aligned} dX_0^{(s)}/dt &= -(\lambda + d)X_0^{(s)} \\ dX_i^{(s)}/dt &= 2\lambda X_{i-1}^{(s)} - (\lambda + d)X_i^{(s)}, \quad i = 1,\ldots,4 \\ dX_{5+}^{(s)}/dt &= 2\lambda(X_4^{(s)} + X_{5+}^{(s)}) - dX_{5+}^{(s)}. \end{aligned} \tag{2}$$

Hereby, the parameter s denotes the subpopulation and is an integer ranging from 1 to the number of subpopulations considered in the model. We assume that at time $t = 0$, all cells are undivided and their number is $\sum_s X_0^{(s)}(0) = 5000$. It is useful to define the initial fraction f_s of undivided cells in the sth subpopulation by $X_0^{(s)}(0) = f_s \sum_s X_0^{(s)}(0)$. Obviously, $\sum_s f_s = 1$. Unlike the models used in Wilson et al. (2008) and van der Wath et al. (2009), this model does not assume that fast-cycling cells arise from dormant cells by differentiation. Rather, we assume that each subpopulation is independently dividing and differentiating.

The most straightforward way to analyze the LKS CFSE cell data would be to successively fit the one-, two-, and three-subpopulation versions of the mathematical model and to assess if increasing the number of subpopulations increases the goodness of fit (as measured by the residual sum of squares) significantly (as determined by an F-test). However, a straightforward fit of a model with more than one subpopulation, in which the parameters of the model are unconstrained, does not result in consistent goodness of fit and consistent parameter estimates. We have therefore adopted a two-step procedure to estimate the parameters of the mathematical models. First, we estimate the differentiation rates d of the first two subpopulations from the normalized cell counts (defined in Eq. 3). This leads to a constraint for the differentiation rates. Second, we estimate the division rates and the differentiation rates of the remaining subpopulations from fitting the model to the LKS cell count in the different division classes.

Normalized cell counts are a way to eliminate the division kinetics from CFSE data (De Boer et al., 2006). The normalized cell count is defined as:

$$N(t) = \sum_{i=0}^{4} X_i(t) / 2^i. \tag{3}$$

Assuming a single, homogeneous subpopulation, $N(t)$ is an exponentially decaying function which is independent of the division rate λ:

$$N(t) = N(0)\, e^{-dt}. \tag{4}$$

Thus, in a plot of $\ln(N(t))$ versus the time, t, the slope is d. Assuming two subpopulations, $N(t)$ is a bimodally decaying function that is independent of the division rates λ_1 and λ_2 :

$$N(t) = N(0)\left(f_1 e^{-d_1 t} + (1 - f_1)e^{-d_2 t}\right). \tag{5}$$

We fitted Eqs. 4 and 5 to the normalized cell counts by minimizing the squared difference between log-transformed normalized cell counts and the predictions of Eqs. 4 and 5. We found that the two-subpopulation model fits significantly better than the one-subpopulation model (F-test, $df_1 = 28$, $df_2 = 26$, $P = 2.2 \times 10^{-4}$). Thus, there is a strong statistical signal that the LKS cell population is heterogeneous with respect to its differentiation rate. The best estimates for the parameters of Eq. 5 are:

$$\begin{aligned} f_1 &= 0.70 \pm 0.06 \\ d_1 &= (1.82 \pm 0.90)\ /\ wk \\ d_2 &= (0.127 \pm 0.022)\ /\ wk. \end{aligned} \tag{6}$$

The death rates correspond to a mean life-span of 3.8 and 55 d, respectively. (Fitting Eq. 4, we obtain $d = (0.254 \pm 0.020)$/wk.)

In the next step, we fitted the full two- and three-subpopulation model and estimated the remaining parameters of these models. The fitting routine involved minimizing the squared difference between log-transformed LKS cell counts and the predictions of the two- or three-subpopulation models. The last division class, five and greater, was omitted in the fitting procedure because we found, on the basis of simulated data, that omitting the last division class resulted in less biased parameter estimates. We found that there is evidence for at least three subpopulations in the data. A three-subpopulation model, assuming Poisson division and loss of LKS cells, fits significantly better than a model assuming two subpopulations (F-test, $df_1 = 153$, $df_2 = 150$, $P = 2.4 \times 10^{-14}$). Estimates of the parameters that characterize the three subpopulations are listed in Table S1. Hereby, f_1, f_2, and f_3 are the initial fractions of subpopulation one, two, and three, respectively. λ_i is the division rate, and d_i is the loss rate of the ith subpopulation (as a result of differentiation, loss of marker, or death). Thus, we have evidence for a subpopulation that is lost at the high rate of $d_1 = 1.8\ /\ wk$ and does not divide. Subpopulations two and three initially constitute 22 and 7.7% of the LKS population and divide once every 12 and 97 d, respectively. Subpopulations two and three correspond to the slowly and fast cycling subpopulations that were identified previously (Wilson et al., 2008; Foudi et al., 2009; van der Wath et al., 2009).

Mathematical modeling and analysis of division kinetics of biologically functional HSC. To estimate the turnover rate of biologically functional HSC from the repopulation data, we first estimated the fraction of biologically functional HSC in the LKS cell population in division class zero and five or higher by a maximum likelihood procedure. If the fraction of biologically functional HSC is f_{HSC}, and we transfer i LKS cells to m mice, the probability to observe repopulation of the hematopoietic system in r mice is:

$$\binom{m}{m-r}\left(1 - f_{HSC}\right)^{i(m-r)}\left(1 - (1 - f_{HSC})^i\right)^r. \tag{7}$$

If we conduct E such repopulation experiments, the best estimate for the fraction of biologically functional HSC in the LKS population maximizes the following likelihood:

$$L(f_{HSC}) = \prod_{k=1}^{E} \binom{m_k}{m_k - r_k}\left(1 - f_{HSC}\right)^{i_k(m_k - r_k)}\left(1 - (1 - f_{HSC})^{i_k}\right)^{r_k}. \tag{8}$$

In this expression, the variables m_k or r_k denote the number of mice used or repopulated in experiment k, respectively, and i_k is the number of LKS cells transferred in experiment k.

We used the repopulation data to estimate the fraction of biologically functional HSC in division classes zero and five or higher at 3, 7, 12, and 14 wk after primary transfer of the LKS cell population. Combining these estimates with the number of LKS cells in each division class, we obtain an estimate

for the number of biologically functional HSC in the division classes zero and five or higher. Table S2 shows these estimates.

We then used the homogeneous cell division model (Eq. 1) to estimate the turnover rate of biologically functional HSC. We assumed that the number of biologically functional HSC stays constant over the 14 wk. This constant number of biologically functional HSCs can be interpreted as the number of stem cell niches that are occupied after the transfer of CFSE-labeled cells. Assuming a constant number of biologically functional HSCs is mathematically equivalent to setting the division rate equal to the rate of differentiation or loss of biologically functional HSC.

We estimated a division rate of 0.18/wk, which corresponds to one division every 39 d. The 95% confidence interval of this estimate is 0.14–0.35/wk, which corresponds to a range of one division every 20–50 d. This is strong evidence that biologically functional HSCs do not divide only every 150 d, as has been suggested by other studies (Wilson et al., 2008; Wilson et al., 2009; Trumpp et al., 2010). The constant number of biologically functional HSCs in the system (i.e., the number of occupied stem cell niches) is estimated as 388 cells (95% confidence interval: 193–559 cells).

We investigated whether relaxing some of the model assumptions alters the estimate of biologically functional HSC dramatically but found that the estimate of the turnover rate is robust. If we relax the assumption that the division rate equals the rate of differentiation and loss, we obtain a division rate of 0.26/wk, which lies within the 95% confidence interval of the estimate assuming equal division and differentiation rates. This means that the two estimates are not significantly different. If we set the number of niches to 200 rather than estimating this quantity from the data, we obtain a division rate of 0.24/wk, which is, again, not significantly different from the estimate based on flexible number of niches. Lastly, a two-population model does not significantly improve the fit to the data on biologically functional HSC (Table S2): F-test, $df_1 = 29$, $df_2 = 27$, $P = 0.15$. Thus, there is no evidence for a heterogeneously dividing population of biologically functional HSC.

Implementation. All the mathematical models and the analysis described in the previous two sections were implemented in the R language of statistical computing (R Development Core Team, 2008).

Online supplemental material. Fig. S1 shows homogenous CFSE labeling and CFSE label–retaining cell populations upon nonconditioned transplantation of LKS but not LK. Fig. S2 shows 0×-divided cells that are maintained in BM, but not spleen, and included in LKS $CD34^-CD150^+$ population. Fig. S3 shows donor contribution to lymphoid lineage in secondary transplantation with 0×- or ≥5×-divided LKS cells, and HSC frequency determined by limiting dilution transplantation. Fig. S4 shows donor chimerism in HSC-containing population in BM of secondary recipient reconstituted with 0–2×- or ≥5×-divided LKS cells. Fig. S5 shows hypothetical models for steady-state hematopoiesis. Table S1 shows estimates of the parameters of the three-subpopulation model on LKS turnover. Table S2 shows estimate of biologically functional HSC. Online supplemental material is available at http://www.jem.org/cgi/content/full/jem.20101643/DC1.

The authors thank D. Jarrossay for FACS sorting, and D. Bossi and C. Borsotti for assistance with some experiments.

This work was supported in part by a Postdoctoral Fellowship of the Japanese Society for the Promotion of Science for Research Abroad to H. Takizawa, the Swiss National Science Foundation (310000-116637), the Oncosuisse (OCS-02019-02-2007), and the Promedica Foundation to M.G. Manz.

The authors declare no competing interest.

Author contributions: H. Takizawa designed research, performed the experiments, and wrote the manuscript; C.S. Boddupalli performed experiments; R.R. Regoes and S. Bonhoeffer generated mathematical models; and M.G. Manz directed the study and wrote the manuscript.

Submitted: 9 August 2010
Accepted: 11 January 2011

REFERENCES

Akashi, K., D. Traver, T. Miyamoto, and I.L. Weissman. 2000. A clonogenic common myeloid progenitor that gives rise to all myeloid lineages. *Nature*. 404:193–197. doi:10.1038/35004599

Allsopp, R.C., S. Cheshier, and I.L. Weissman. 2001. Telomere shortening accompanies increased cell cycle activity during serial transplantation of hematopoietic stem cells. *J. Exp. Med.* 193:917–924. doi:10.1084/jem.193.8.917

Allsopp, R.C., G.B. Morin, R. DePinho, C.B. Harley, and I.L. Weissman. 2003. Telomerase is required to slow telomere shortening and extend replicative lifespan of HSCs during serial transplantation. *Blood*. 102:517–520. doi:10.1182/blood-2002-07-2334

Baldridge, M.T., K.Y. King, N.C. Boles, D.C. Weksberg, and M.A. Goodell. 2010. Quiescent haematopoietic stem cells are activated by IFN-gamma in response to chronic infection. *Nature*. 465:793–797. doi:10.1038/nature09135

Bhattacharya, D., D.J. Rossi, D. Bryder, and I.L. Weissman. 2006. Purified hematopoietic stem cell engraftment of rare niches corrects severe lymphoid deficiencies without host conditioning. *J. Exp. Med.* 203:73–85. doi:10.1084/jem.20051714

Bhattacharya, D., A. Czechowicz, A.G. Ooi, D.J. Rossi, D. Bryder, and I.L. Weissman. 2009. Niche recycling through division-independent egress of hematopoietic stem cells. *J. Exp. Med.* 206:2837–2850. doi:10.1084/jem.20090778

Cheshier, S.H., S.J. Morrison, X. Liao, and I.L. Weissman. 1999. In vivo proliferation and cell cycle kinetics of long-term self-renewing hematopoietic stem cells. *Proc. Natl. Acad. Sci. USA*. 96:3120–3125. doi:10.1073/pnas.96.6.3120

Christensen, J.L., and I.L. Weissman. 2001. Flk-2 is a marker in hematopoietic stem cell differentiation: a simple method to isolate long-term stem cells. *Proc. Natl. Acad. Sci. USA*. 98:14541–14546. doi:10.1073/pnas.261562798

De Boer, R.J., V.V. Ganusov, D. Milutinoviç, P.D. Hodgkin, and A.S. Perelson. 2006. Estimating lymphocyte division and death rates from CFSE data. *Bull. Math. Biol.* 68:1011–1031. doi:10.1007/s11538-006-9094-8

Drize, N.J., J.R. Keller, and J.L. Chertkov. 1996. Local clonal analysis of the hematopoietic system shows that multiple small short-living clones maintain life-long hematopoiesis in reconstituted mice. *Blood*. 88:2927–2938.

Essers, M.A., S. Offner, W.E. Blanco-Bose, Z. Waibler, U. Kalinke, M.A. Duchosal, and A. Trumpp. 2009. IFNalpha activates dormant haematopoietic stem cells in vivo. *Nature*. 458:904–908. doi:10.1038/nature07815

Foudi, A., K. Hochedlinger, D. Van Buren, J.W. Schindler, R. Jaenisch, V. Carey, and H. Hock. 2009. Analysis of histone 2B-GFP retention reveals slowly cycling hematopoietic stem cells. *Nat. Biotechnol.* 27:84–90. doi:10.1038/nbt.1517

Glauche, I., K. Moore, L. Thielecke, K. Horn, M. Loeffler, and I. Roeder. 2009. Stem cell proliferation and quiescence—two sides of the same coin. *PLOS Comput. Biol.* 5:e1000447. doi:10.1371/journal.pcbi.1000447

Gordon, M.Y., J.L. Lewis, and S.B. Marley. 2002. Of mice and men...and elephants. *Blood*. 100:4679–4680. doi:10.1182/blood-2002-08-2517

Harrison, D.E., and C.M. Astle. 1982. Loss of stem cell repopulating ability upon transplantation. Effects of donor age, cell number, and transplantation procedure. *J. Exp. Med.* 156:1767–1779. doi:10.1084/jem.156.6.1767

Jordan, C.T., and I.R. Lemischka. 1990. Clonal and systemic analysis of long-term hematopoiesis in the mouse. *Genes Dev.* 4:220–232. doi:10.1101/gad.4.2.220

Karsunky, H., M. Merad, A. Cozzio, I.L. Weissman, and M.G. Manz. 2003. Flt3 ligand regulates dendritic cell development from $Flt3^+$ lymphoid and myeloid-committed progenitors to $Flt3^+$ dendritic cells in vivo. *J. Exp. Med.* 198:305–313. doi:10.1084/jem.20030323

Kay, H.E. 1965. How many cell-generations? *Lancet*. 286:418–419. doi:10.1016/S0140-6736(65)90763-4

Kiel, M.J., O.H. Yilmaz, T. Iwashita, O.H. Yilmaz, C. Terhorst, and S.J. Morrison. 2005. SLAM family receptors distinguish hematopoietic stem and progenitor cells and reveal endothelial niches for stem cells. *Cell*. 121:1109–1121. doi:10.1016/j.cell.2005.05.026

Kiel, M.J., S. He, R. Ashkenazi, S.N. Gentry, M. Teta, J.A. Kushner, T.L. Jackson, and S.J. Morrison. 2007. Haematopoietic stem cells do not asymmetrically segregate chromosomes or retain BrdU. *Nature*. 449:238–242. doi:10.1038/nature06115

Kondo, M., I.L. Weissman, and K. Akashi. 1997. Identification of clonogenic common lymphoid progenitors in mouse bone marrow. *Cell*. 91:661–672. doi:10.1016/S0092-8674(00)80453-5

Kondo, M., A.J. Wagers, M.G. Manz, S.S. Prohaska, D.C. Scherer, G.F. Beilhack, J.A. Shizuru, and I.L. Weissman. 2003. Biology of hematopoietic stem cells and progenitors: implications for clinical application. *Annu. Rev. Immunol.* 21:759–806. doi:10.1146/annurev.immunol.21.120601.141007

Lemischka, I.R., D.H. Raulet, and R.C. Mulligan. 1986. Developmental potential and dynamic behavior of hematopoietic stem cells. *Cell*. 45:917–927. doi:10.1016/0092-8674(86)90566-0

Lyons, A.B., and C.R. Parish. 1994. Determination of lymphocyte division by flow cytometry. *J. Immunol. Methods*. 171:131–137. doi:10.1016/0022-1759(94)90236-4

Massberg, S., P. Schaerli, I. Knezevic-Maramica, M. Köllnberger, N. Tubo, E.A. Moseman, I.V. Huff, T. Junt, A.J. Wagers, I.B. Mazo, and U.H. von Andrian. 2007. Immunosurveillance by hematopoietic progenitor cells trafficking through blood, lymph, and peripheral tissues. *Cell*. 131:994–1008. doi:10.1016/j.cell.2007.09.047

McKenzie, J.L., O.I. Gan, M. Doedens, J.C. Wang, and J.E. Dick. 2006. Individual stem cells with highly variable proliferation and self-renewal properties comprise the human hematopoietic stem cell compartment. *Nat. Immunol.* 7:1225–1233. doi:10.1038/ni1393

Méndez-Ferrer, S., D. Lucas, M. Battista, and P.S. Frenette. 2008. Haematopoietic stem cell release is regulated by circadian oscillations. *Nature*. 452:442–447. doi:10.1038/nature06685

Morita, Y., H. Ema, and H. Nakauchi. 2010. Heterogeneity and hierarchy within the most primitive hematopoietic stem cell compartment. *J. Exp. Med*. 207:1173–1182. doi:10.1084/jem.20091318

Nagai, Y., K.P. Garrett, S. Ohta, U. Bahrun, T. Kouro, S. Akira, K. Takatsu, and P.W. Kincade. 2006. Toll-like receptors on hematopoietic progenitor cells stimulate innate immune system replenishment. *Immunity*. 24:801–812. doi:10.1016/j.immuni.2006.04.008

Nygren, J.M., and D. Bryder. 2008. A novel assay to trace proliferation history in vivo reveals that enhanced divisional kinetics accompany loss of hematopoietic stem cell self-renewal. *PLoS One*. 3:e3710. doi:10.1371/journal.pone.0003710

Onai, N., A. Obata-Onai, M.A. Schmid, T. Ohteki, D. Jarrossay, and M.G. Manz. 2007. Identification of clonogenic common Flt3+M-CSFR+ plasmacytoid and conventional dendritic cell progenitors in mouse bone marrow. *Nat. Immunol.* 8:1207–1216. doi:10.1038/ni1518

Orford, K.W., and D.T. Scadden. 2008. Deconstructing stem cell self-renewal: genetic insights into cell-cycle regulation. *Nat. Rev. Genet*. 9:115–128. doi:10.1038/nrg2269

Osawa, M., K. Hanada, H. Hamada, and H. Nakauchi. 1996a. Long-term lymphohematopoietic reconstitution by a single CD34-low/negative hematopoietic stem cell. *Science*. 273:242–245. doi:10.1126/science.273.5272.242

Osawa, M., K. Nakamura, N. Nishi, N. Takahasi, Y. Tokuomoto, H. Inoue, and H. Nakauchi. 1996b. In vivo self-renewal of c-Kit+ Sca-1+ Lin(low/-) hemopoietic stem cells. *J. Immunol.* 156:3207–3214.

Qian, H., N. Buza-Vidas, C.D. Hyland, C.T. Jensen, J. Antonchuk, R. Månsson, L.A. Thoren, M. Ekblom, W.S. Alexander, and S.E. Jacobsen. 2007. Critical role of thrombopoietin in maintaining adult quiescent hematopoietic stem cells. *Cell Stem Cell*. 1:671–684. doi:10.1016/j.stem.2007.10.008

R Development Core Team. 2008. R: A language and environment for statistical computing. *In* R Foundation for Statistical Computing, Vienna, Austria. www.r-project.org.

Rakoff-Nahoum, S., and R. Medzhitov. 2009. Toll-like receptors and cancer. *Nat. Rev. Cancer*. 9:57–63. doi:10.1038/nrc2541

Rufer, N., T.H. Brümmendorf, S. Kolvraa, C. Bischoff, K. Christensen, L. Wadsworth, M. Schulzer, and P.M. Lansdorp. 1999. Telomere fluorescence measurements in granulocytes and T lymphocyte subsets point to a high turnover of hematopoietic stem cells and memory T cells in early childhood. *J. Exp. Med*. 190:157–167. doi:10.1084/jem.190.2.157

Sato, T., N. Onai, H. Yoshihara, F. Arai, T. Suda, and T. Ohteki. 2009. Interferon regulatory factor-2 protects quiescent hematopoietic stem cells from type I interferon-dependent exhaustion. *Nat. Med*. 15:696–700. doi:10.1038/nm.1973

Smith, L.G., I.L. Weissman, and S. Heimfeld. 1991. Clonal analysis of hematopoietic stem-cell differentiation in vivo. *Proc. Natl. Acad. Sci. USA*. 88:2788–2792. doi:10.1073/pnas.88.7.2788

Spangrude, G.J., S. Heimfeld, and I.L. Weissman. 1988. Purification and characterization of mouse hematopoietic stem cells. *Science*. 241:58–62. doi:10.1126/science.2898810

Trumpp, A., M. Essers, and A. Wilson. 2010. Awakening dormant haematopoietic stem cells. *Nat. Rev. Immunol.* 10:201–209. doi:10.1038/nri2726

van der Wath, R.C., A. Wilson, E. Laurenti, A. Trumpp, and P. Liò. 2009. Estimating dormant and active hematopoietic stem cell kinetics through extensive modeling of bromodeoxyuridine label-retaining cell dynamics. *PLoS One*. 4:e6972. doi:10.1371/journal.pone.0006972

Weksberg, D.C., S.M. Chambers, N.C. Boles, and M.A. Goodell. 2008. CD150 side population cells represent a functionally distinct population of long-term hematopoietic stem cells. *Blood*. 111:2444–2451. doi:10.1182/blood-2007-09-115006

Weston, S.A., and C.R. Parish. 1990. New fluorescent dyes for lymphocyte migration studies. Analysis by flow cytometry and fluorescence microscopy. *J. Immunol. Methods*. 133:87–97. doi:10.1016/0022-1759(90)90322-M

Wilson, A., E. Laurenti, G. Oser, R.C. van der Wath, W. Blanco-Bose, M. Jaworski, S. Offner, C.F. Dunant, L. Eshkind, E. Bockamp, et al. 2008. Hematopoietic stem cells reversibly switch from dormancy to self-renewal during homeostasis and repair. *Cell*. 135:1118–1129. doi:10.1016/j.cell.2008.10.048

Wilson, A., E. Laurenti, and A. Trumpp. 2009. Balancing dormant and self-renewing hematopoietic stem cells. *Curr. Opin. Genet. Dev.* 19:461–468. doi:10.1016/j.gde.2009.08.005

Wright, D.E., A.J. Wagers, A.P. Gulati, F.L. Johnson, and I.L. Weissman. 2001. Physiological migration of hematopoietic stem and progenitor cells. *Science*. 294:1933–1936. doi:10.1126/science.1064081

Yoshihara, H., F. Arai, K. Hosokawa, T. Hagiwara, K. Takubo, Y. Nakamura, Y. Gomei, H. Iwasaki, S. Matsuoka, K. Miyamoto, et al. 2007. Thrombopoietin/MPL signaling regulates hematopoietic stem cell quiescence and interaction with the osteoblastic niche. *Cell Stem Cell*. 1:685–697. doi:10.1016/j.stem.2007.10.020